

Solventless green synthesis of 4-*O*-aryloxy carbonates from aryl/alkyl-oxy propanediols and dimethyl carbonate over nano-crystalline alkali promoted alkaline earth metal oxides†

Ganapati D. Yadav* and Prasad S. Surve

Cite this: *Catal. Sci. Technol.*, 2013, **3**, 2668

4-*O*-(Alkyl/aryl)-oxy-1,3-dioxolane-2-ones find wide applications such as additives, solvents in lithium ion batteries and building blocks in the synthesis of chiral oxazolidinone derivatives. Traditional processes to synthesize 4-*O*-(alkyl/aryl)-oxy-1,3-dioxolan-2-ones include the use of isocyanates and phosgene derivatives as carbonylating agents which are very toxic, highly hazardous and require longer reaction times. In the present work, a green and solventless process was developed to synthesize 4-*O*-(aryl/alkyl)-oxy-1,3-dioxolan-2-ones by reacting 3-(aryl/alkyl)-oxy-1,2-propanediol with dimethyl carbonate using alkali promoted MgO catalyst prepared by a combustion synthesis (CS) method. The self propagating CS method is the most effective to prepare highly active oxide nanoparticles considering the cost of synthesis and simplicity. A series of alkali promoted MgO catalysts with different alkali promoters were prepared using the CS method. Catalysts with different alkali promoters were screened to study their efficacy, among which lithium metal was found to be the best promoter with 0.1% as optimum loading on MgO. The resulting catalysts were characterized by CO₂-TPD, FTIR, XRD, BET, etc. The effects of various parameters such as molar ratio, speed of agitation, catalyst loading and temperature were studied. The reaction mechanism followed a Langmuir–Hinshelwood–Hougen–Watson (LHHW) model with strong adsorption of both reactants leading to zero order kinetics with 28 kcal mol⁻¹ as the apparent activation energy. Complete conversion of 3-*O*-(aryl/alkyl)-oxy-1,2-propanediol with 100% selectivity towards 4-*O*-(aryl/alkyl)-oxy carbonates was achieved with different aryl/alkyl substituents. The process gave 88.66% atom economy with an *E*-factor of 0.3 in 1 h at 140 °C.

Received 27th March 2013,
Accepted 27th June 2013

DOI: 10.1039/c3cy00204g

www.rsc.org/catalysis

Introduction

The 4-*O*-(aryl/alkyl)-oxy-1,3-dioxolan-2-one family of chemicals are important building blocks in the pharmaceutical industry; they are used in the synthesis of chiral inhibitor analogs of monoamine oxidase, the degradation of various amine neurotransmitters;¹ and the synthesis of chiral oxazolidinones used as antidepressants, for mood disorders, as psychopharmacologic drugs, as smoking cessation agents, as aids for treatment of poisoning, drug abuse and dependency, and as monoamine oxidase inhibitors;^{2–7} as well as in the synthesis of carbamates which show anticonvulsant activity. They are used as additives/solvent in lithium ion batteries to improve their power characteristics, and some derivatives have been used as muscle relaxants and have widely been used as insecticides.⁸

Department of Chemical Engineering, Institute of Chemical Technology, Matunga, Mumbai-400 019, India. E-mail: gdyadav@yahoo.com, surveps@gmail.com;
Fax: +91-22-3361-1002, +91-22-3361-1020; Tel: +91-22-3361-1001

† Electronic supplementary information (ESI) available. See DOI: 10.1039/c3cy00204g

Traditional processes to synthesize 4-*O*-(alkyl/aryl)-oxy-1,3-dioxolan-2-one include the reaction between 3-aryloxy-1,2-propanediol with hazardous reagents such as isocyanate, phosgene or triphosgene.^{9–11} It is also prepared by using basic condensation homogeneous catalysts such as alkali metal carbonates, bicarbonates and acetates, alkali metal alcoholates and hydroxides.^{12–15} Ming-Shiu *et al.* synthesized 4-phenoxyethyl-1,3-dioxolane-2-one by reacting phenyl glycidyl ether and diphenyl carbonate using a quaternary ammonium salt as a catalyst.¹⁶ It has also been prepared by reacting epoxides or glycidyl ether with CO₂ in the presence of hydrotalcite.¹⁷ All the above processes suffer from the use of hazardous reactants, harsh reaction conditions and require additional purification steps, thereby increasing the cost of production.

Several methods have been developed to convert diols to their carbonate derivatives by reacting with dialkyl carbonates using heterogeneous base catalysts.^{18–20} From the green and sustainable chemistry point of view, it is desirable to develop a neat process using a heterogeneous catalyst with fewer steps, easier separation, reusability, high selectivity and yield, milder

reaction conditions and the use of less hazardous, non toxic reagents. Combustion synthesis (CS) leads to very interesting characteristics of inorganic oxides, which could be further modified to endow them with interesting catalytic properties. It is a self propagating high temperature synthesis and an effective and low cost method for the synthesis of materials.^{21–24} In our laboratory, both strongly acidic and basic catalysts have been prepared recently using combustion synthesis.^{24–26}

In the present work, 4-*O*-(aryl/alkyl)-oxy-1,3-dioxolane-2-one was synthesized by reacting 3-(aryl/alkyl)-oxy-1,2-propanediol with dimethyl carbonate using a lithium promoted MgO catalyst prepared by a CS method. The catalytic activity of MgO was found to be increased by promotion with alkali metal salts and can be used for several reactions such as condensation, oxidative coupling, *O*-alkylation, *etc.*^{27–33} Alkali metal ion promoted MgO catalysts are conventionally prepared by the co-precipitation method, which is a tedious and low yielding process. Self propagating combustion synthesis offers the best method to prepare highly active oxide nano-particles with low cost and ease of synthesis.^{34–36} A series of alkali promoted MgO with different alkali promoters were prepared using the CS method. Lithium promoted MgO with different amounts of Li loading was also prepared. The resulting catalysts were characterized by CO₂-TPD (temperature programmed desorption), FTIR, XRD, BET, *etc.* Their catalytic activity was tested in the synthesis of 4-*O*-(aryl/alkyl)-oxy-1,3-dioxolane-2-one. The overall process is clean and green.

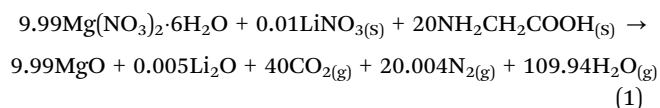
Experimental

Chemicals and catalysts

All chemicals were procured from reputed firms: magnesium nitrate hexahydrate, lithium nitrate, glycine, dimethyl carbonate, *n*-decane were obtained from M/s. s.d. Fine Chemicals Pvt. Ltd., Mumbai, India. 3-Aryloxy-1,2-propanediols were synthesized by a procedure reported by Egri *et al.*³⁷ and purified by recrystallization to achieve 98% purity.

Synthesis of catalyst

Nano-crystalline alkali promoted MgO was synthesized by a typical solution combustion technique,³⁴ where predetermined quantities of glycine (as fuel), magnesium nitrate hexahydrate and lithium nitrate (as oxidizer) were dissolved in a minimum amount of water. The fuel to oxidizer ratio (F/O) was taken as 2, as shown in eqn (1). The mixture containing fuel and oxidizer was taken in a silica crucible and heated to form a highly viscous gel. This viscous gel was then transferred into a muffle furnace preheated at 350 °C, which underwent dehydration followed by smoldering combustion leading to a large volume of nanocrystalline brown colored material. This material was then calcined at 500 °C for 3 h to remove unwanted carbon and to achieve a white fluffy nanocrystalline powder. The theoretical equation considering F/O = 2 can be shown as³⁴



Catalyst characterization

Powder X-ray diffraction patterns of Li metal promoted MgO with different Li metal loadings were determined on a Bruker AXS, D8 Discover instrument (USA) using Cu-K α radiation at $\lambda = 1.5406 \text{ \AA}$ from $2\theta = 10$ to 90° with a scan step of 1 s and a step size of 0.1.

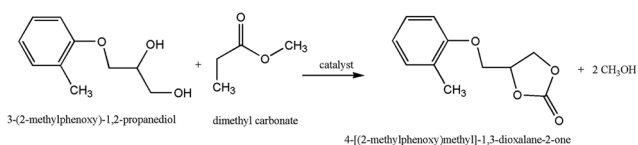
FTIR studies were carried by using PerkinElmer Turbomass ver 5.0.0 to identify the chemical nature of the adsorbed surface CO₂ species. The series of Li loaded samples were allowed to adsorb CO₂ at room temperature.

CO₂-temperature programmed desorption (TPD) studies were performed to determine catalyst base site densities in an Autochem II (Micromeritics, USA) instrument equipped with a TCD detector. Approximately 0.2 g of catalyst was loaded in the sample holder and heated at 823 K in nitrogen and subsequently cooled to 298 K. After dosing with 10 vol% CO₂ in helium mixture at a flow rate of 20 ml min⁻¹ for 30 min, the system was purged with nitrogen for 1 h at the same temperature. The physisorbed CO₂ was removed by passing helium gas at room temperature for 30 min. After cooling at 298 K the temperature was raised to 823 K at the rate of 303 K per min and the desorbed CO₂ was analyzed by TCD.

The surface morphology of the sample was determined by scanning electron microscopy (SEM) using a JEOL JSM 7400 microscope operated at 20 kV with a working distance of 10 mm and resolution of up to 10 nm. Dried samples were mounted on specimen studs and sputter coated with a thin film of platinum to prevent charging. The platinum coated surface was then scanned at various magnifications using a scanning electron microscope. BET surface area and pore volume was determined by BJH and multipoint BET method by using a Micromeritics ASAP-2010 instrument. The analysis was carried out at 77 K maintained by liquid nitrogen, after preheating the sample at 200 °C for 2 h. TEM images of the sample were obtained with a JEOL 3010 instrument with a UHR polar piece.

Reaction procedure

Reactions were carried out in an autoclave with a 100 cm³ capacity (Amar Equipments, Mumbai, India), equipped with a four-bladed pitched-turbine impeller along with temperature controller, speed controller and pressure indicator. In a typical experiment (Scheme 1) the autoclave was charged with reaction mixture consisting of 0.02 mol 3-(2-methylphenoxy)-1,2-propanediol, 0.3 mol dimethyl carbonate, internal standard (*n*-decane) and a catalyst loading 0.03 g cm⁻³ of total reaction volume. The catalyst was activated at 573 K under nitrogen flow for 4 h prior to use. The temperature was raised and maintained at ± 1 °C of the set value with the help of an in-built proportional integral derivative (PID) controller. Once the



Scheme 1 Reaction scheme.

temperature reached the desired value, agitation was started. Then, an initial sample was withdrawn and further samples were drawn at periodic intervals up to 1 h. The temperature was maintained at 140 °C and the speed of agitation at 1000 rpm. The reaction was carried out without the use of any solvent. The total volume of the liquid phase was 30 cm³.

Analysis of reaction mixture

The samples were analyzed using GC (Chemito Ceres800 model) equipped with a 30 m × 0.25 mm i.d. BPX-5 capillary column and flame ionization detector (FID). Reaction products were confirmed by GC-MS (PerkinElmer Clarus 500). Reaction products were purified by filtering solid catalyst followed by vacuum distillation to remove excess DMC and methanol. Purified products were dissolved in CDCl₃ and were analysed by 400 MHz Bruker ¹H NMR spectroscopy.

Results and discussion

Catalyst characterization

The effect of different alkali promoters showed that the highest catalytic activity was obtained when lithium was used as a promoter, which is in complete agreement with the reported results.³² Detailed catalyst characterization was carried out for lithium promoted magnesium oxide.

XRD studies

The powder X-ray diffraction patterns of Li promoted MgO with different Li loading are shown in Fig. 1. The samples with lithium loading of less than 0.5 wt% exhibit a completely crystalline cubic phase and all diffraction peaks show a single phase of MgO (JCPDS card No. 87-0652) periclase with characteristic peaks at 2θ values of 37.1°, 42.8° and 62.4°, which confirms the formation of a nanocrystalline homogeneous powder with a rock salt structure. There is no significant change in unit cell parameter values for Li promoted MgO calculated from diffractograms, which suggests no detectable modification in the MgO lattice by Li doping of less than 0.5 wt%.

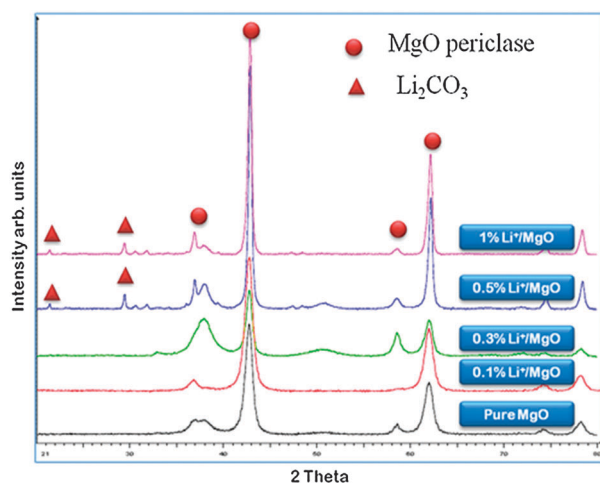


Fig. 1 XRD analysis of Li promoted MgO.

Table 1 Effect of lithium loading particle size and surface area

Sr. no.	Li ⁺ loading wt%	Particle size ^a	Surface area	Conversion	Selectivity
1	0	9	205	49	100
2	0.1	9.03	181	100	100
3	0.3	11.71	117	83	100
4	0.5	20.93	95.25	76	100

Reaction conditions: 3-(*O*-methylphenoxy)-1,2-propanediol: 3.6 g (0.02 mol); dimethyl carbonate: 27.04 g (0.3 mol); reaction temperature: 140 °C; catalyst loading: 0.03 g cm⁻³; speed: 1000 rpm; reaction time: 1 h. ^a From Scherer's equation.

However, crystalline Li containing the Li₂CO₃ phase (JCPDS card No. 22-1141) was observed in the 0.5 wt% Li promoted MgO sample. The samples with a Li content of less than 0.5% are in the form of Li₂O (JCPDS card No. 12-0254), which can be seen for the 0.3% Li/MgO sample observed at 33°.

The crystalline size of combustion synthesized pure MgO and Li promoted MgO was calculated using Scherer's equation, considering the width of the main MgO reflection at 2θ = 42.8°, and the results are summarized in Table 1. As described in the conventional synthesis method, the crystalline size of Li promoted MgO increases with increasing Li loading³² and this effect is consistent in the combustion synthesis method too. However, the broadening of the XRD peaks confirms the nanocrystalline nature of combustion synthesized lithium promoted MgO.

FTIR analysis

FTIR studies were performed to identify the nature of the species on the surface of the catalyst. The nature of the adsorbed species observed in this work is the same as that explained by Díez *et al.*³² Fig. 2 shows the FTIR spectra of 0.1% and 0.5% lithium promoted MgO, which show the presence of unidentate carbonate, bidentate carbonate and bicarbonate species. Symmetric O–C–O stretching at 1360–1400 cm⁻¹ and asymmetric O–C–O stretching at 1510–1560 cm⁻¹ is low. Coordination O²⁻ anions are present at the corners forming unidentate carbonate species.

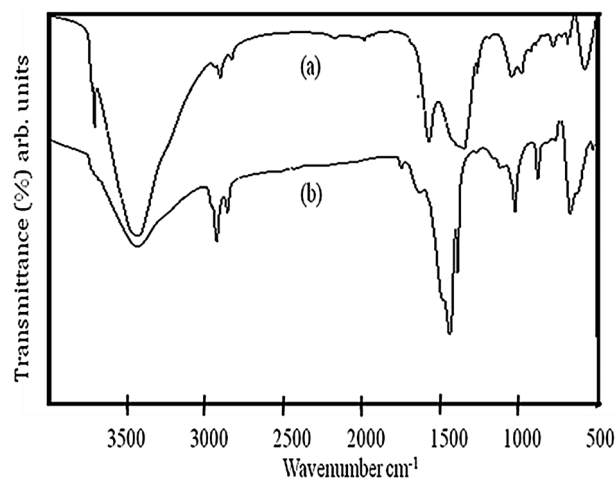


Fig. 2 FTIR spectra of 0.1% and 0.5% lithium promoted MgO, (a) 0.1% LM, (b) 0.5% LM.

Symmetric O–C–O stretching at 1320–1340 cm^{-1} and asymmetric O–C–O stretching at 1610–1630 cm^{-1} are due to Lewis acid–Brønsted base pairs such as $\text{Mg}^{2+}/\text{Li}^+$ and O^{2-} , which form bidentate carbonate species. Peaks for the C–OH bending vibration at 1220 cm^{-1} are due to surface hydroxyl groups which form bicarbonate species and also give symmetric O–C–O stretching at 1480 cm^{-1} and asymmetric O–C–O stretching at 1650 cm^{-1} .

Basicity measurement by CO_2 -TPD

CO_2 -TPD analysis was performed to determine the strength and surface nature of basic sites. CO_2 -TPD profiles of pure MgO and lithium promoted MgO with different lithium ion loadings show the presence of different basic sites of different strengths in different temperature regions (Fig. 3). According to the observed data these sites were differentiated in three different temperature regions as 50–150 $^\circ\text{C}$ for weakly basic sites, 150–450 $^\circ\text{C}$ for medium basic sites and 450–750 $^\circ\text{C}$ for strongly basic sites. Table 2 shows quantified basicity values for each type of basic site described above. These are in agreement with the previous work,²⁸ wherein the peaks in the temperature region 50–150 $^\circ\text{C}$ correspond to weakly basic sites and are attributed to bicarbonate species formed on weakly basic surface hydroxyl groups. The peak in the temperature region 150–450 $^\circ\text{C}$ corresponds to medium basic sites which are due to bidentate carbonate species forming on the metal–oxygen ion pair, and peaks in the temperature range 450–750 $^\circ\text{C}$, corresponding to strongly basic sites, are attributed to unidentate carbonate species formed on low co-ordinate oxygen anions.

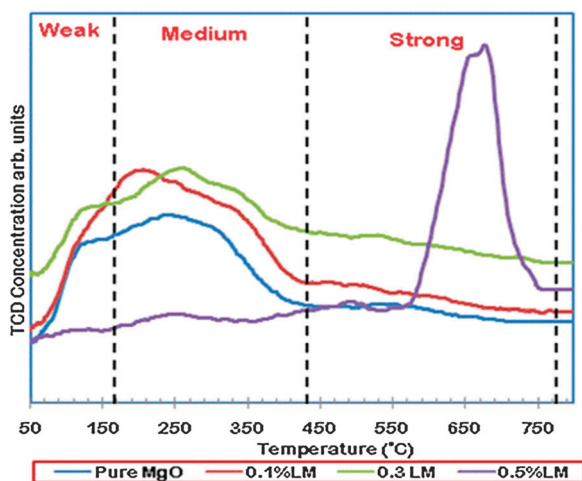


Fig. 3 CO_2 -TPD profiles of pure MgO and lithium promoted MgO with different lithium loadings.

Table 2 CO_2 -TPD basicity values of lithium promoted MgO

Samples	Basicity (mmol g^{-1})			
	Total	Weak	Medium	Strong
Pure MgO	0.73	0.13	0.49	0.11
0.1% LM	0.75	0.13	0.55	0.061
0.3% LM	0.78	0.12	0.51	0.14
0.5% LM	0.34	0.02	0.036	0.28

As the lithium loading increases, total basicity increases. In the case of 0.1% and 0.3% lithium ion loading, a consistent increase in weak and medium basic sites were observed. However, in the case of 0.5% lithium loading, very few weak and medium basic sites were found. In 0.5% lithium ion loaded MgO catalyst, a peak in strong sites at around 650 $^\circ\text{C}$ was observed, which is due to decomposition of lithium carbonate species; which is also seen in XRD studies.

Scanning electron microscopy

The SEM micrographs of lithium promoted MgO with different Li loadings are shown in Fig. 4. These micrographs show the highly porous and spongy nature of lithium promoted MgO. The spongy nature is due to evolution of a large amount of gas during combustion synthesis. Although particle agglomeration is observed in the SEM micrograph of 0.5% lithium promoted MgO as explained in XRD (Fig. 1), particle size increases with increasing Li loading.

BET surface area and pore size analysis

The textural characterization of pure MgO as well as lithium ion promoted MgO prepared by CS method with different lithium ion loadings was determined by nitrogen BJH surface area and pore volume analysis (Table 3). The BET surface area of pure magnesium oxide prepared by CS method is higher than that of

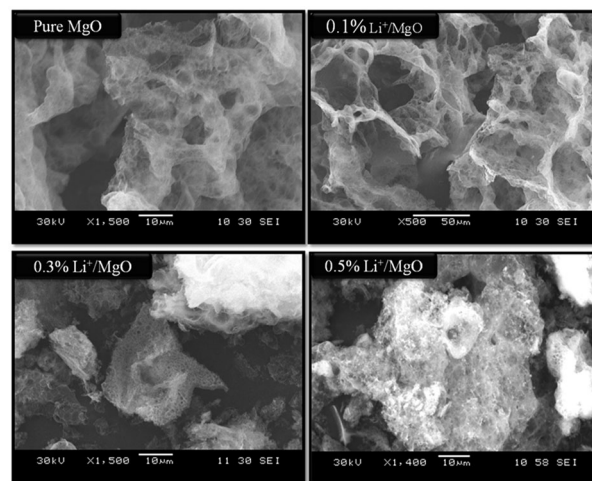


Fig. 4 SEM micrographs of lithium promoted MgO.

Table 3 Effect of different alkali metal ion promoter on particle size and surface area

Sr. no.	Alkali promoter	Particle size	Surface area	Conversion	Selectivity
1	Pure MgO	9	205	49	100
2	Li^+	9.03	181	100	100
3	Na^+	15.84	115	96	100
4	K^+	10.58	146	91	100
5	Cs^+	13.66	85	89	100

Reaction conditions: 3-(*O*-methylphenoxy)-1,2-propanediol: 3.6 g (0.02 mol); dimethyl carbonate: 27.04 g (0.3 mol); reaction temperature: 140 $^\circ\text{C}$; catalyst loading: 0.03 g cm^{-3} ; speed: 1000 rpm; reaction time: 1 h.

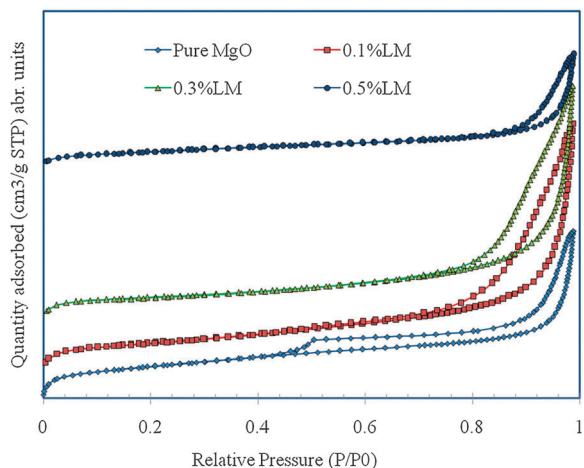


Fig. 5 N_2 adsorption-desorption isotherms with different lithium loadings.

lithium ion loaded MgO. It was observed that as the lithium ion loading increases the BET surface area is decreased. The decrease in surface area may be due to the formation of lithium carbonate species which block the pores. Adsorption-desorption isotherms for all the samples show that they have a type IV isotherm with an H3 hysteresis loop (Fig. 5), which is characteristic of mesoporous materials.

Effect of different alkali metal promoters

The effect of various alkali ion promoters on the conversion of 3-(2-methylphenoxy)-1,2-propanediol to its cyclic carbonate derivatives was studied. The catalyst was prepared by the CS method as described above with alkali metal ion to MgO mole ratio of 0.027 (Table 3). Alkali promoted MgO is found to be superior to pure MgO. Among different promoters, Li^+ ion gives complete conversion of 3-(2-methylphenoxy)-1,2-propanediol, whereas going down the group from lithium to cesium, a slight decrease in conversion was observed. No difference in selectivity was found. Basicity increases from Li_2O to Cs_2O , because the size of the atom also increases, which forms bulky species such as K_2O , Cs_2O and blocks the pores resulting in a decrease in surface area and conversion.³² Hence lithium was used as a promoter for further studies.

Effect of lithium loading

The catalytic activity of lithium promoted MgO with different lithium loadings was tested in the synthesis of 4-[(2-methylphenoxy)methyl]-1,3-dioxolan-2-one to understand the surface base properties. The results shown in Table 1 indicate that rate of reaction is increased by promoting MgO with Li. This is due to the localization of Li_2O species on the surface in the form of $Li_2^+O^-$ groups, which increases local electronegativity and the ability of the catalyst to abstract a proton from 3-(2-methylphenoxy)-1,2-propanediol, followed by bond formation with the carbonyl group of dimethyl carbonate.

The highest catalytic activity was obtained with 0.1% lithium promoted MgO (Table 3), whereas above 0.1 wt%, catalytic activity decreased which may be due to a decrease in the surface area and an increase in the crystalline size, as described above.

Catalytic activity of 0.1% Li/MgO prepared by the CS method is also compared with that of the catalyst prepared by impregnation techniques using commercial MgO sample and lithium nitrate as the precursor, which gave a 68% conversion of 3-(2-methylphenoxy)-1,2-propanediol under similar reaction conditions. Hence further experiments were conducted with 0.1% lithium promoted MgO catalyst prepared by the CS method.

Effect of speed of agitation

The effect of speed of agitation was studied in the range of 800–1200 rpm with 0.03 g cm^{-3} catalyst loading at $140\text{ }^\circ\text{C}$ (Fig. 6). There was no significant change in the rate and conversion patterns, which indicated the absence of any resistance to external mass transfer of reactants to the external surface of the catalysts. All further reactions were carried out at 1000 rpm. A theoretical analysis was also performed as per our previous work to conclude that there was no external mass transfer resistance.^{38–43}

Effect of catalyst loading

The effect of catalyst loading was studied over the range of $0.01\text{--}0.03\text{ g cm}^{-3}$ (Fig. 7). In the absence of external mass transfer resistance, the rate of reaction was directly proportional to catalyst loading based on the entire liquid phase volume. This indicated that as the catalyst loading increased the conversion of

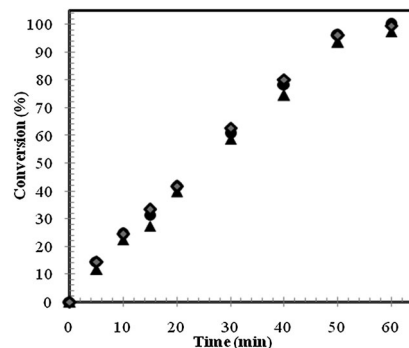


Fig. 6 Effect of speed of agitation. 3-(O-Methylphenoxy)-1,2-propanediol: 3.6 g (0.02 mol); dimethyl carbonate: 27.04 g (0.3 mol); reaction temperature: $140\text{ }^\circ\text{C}$; catalyst loading: 0.03 g cm^{-3} , \blacktriangle 600 rpm, \bullet 800 rpm; \blacklozenge 1000 rpm.

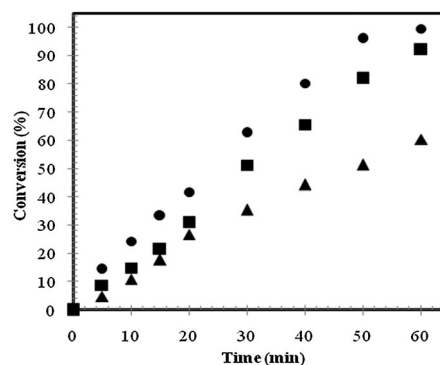


Fig. 7 Effect of catalyst loading. 3-(O-Methylphenoxy)-1,2-propanediol: 3.6 g (0.02 mol); dimethyl carbonate: 27.04 g (0.3 mol); reaction temperature: $140\text{ }^\circ\text{C}$; speed: 1000 rpm, \blacktriangle 0.01 g cm^{-3} , \blacksquare 0.02 g cm^{-3} , \bullet 0.03 g cm^{-3} .

3-aryloxy-1,2-propanediol increased, which was due to a proportionate increase in the number of active sites on the catalyst surface. All further experiments were carried out at 0.03 g cm^{-3} catalyst loading.

Effect of molar ratio

The effect of the molar ratio of 3-(2-methylphenoxy)-1,2-propanediol to dimethyl carbonate was studied from 1:6 to 1:15 under otherwise similar conditions. As the concentration of dimethyl carbonate increased, the conversion as well as the rate of reaction increased (Fig. 8). Considering the solubility of reactants and products formed in the reaction to have a homogeneous liquid phase, further studies were carried out at a 1:15 mole ratio.

Effect of temperature

The effect of temperature on the conversion was studied in the range of 120–140 °C under otherwise similar conditions (Fig. 9). It was observed that the conversion increased with temperature. This would suggest a kinetically controlled mechanism. This is discussed again in the following section.

Reaction mechanism and kinetics

From the observed initial rate, it is evident that the rate is independent of the external mass transfer effects. Thus, the

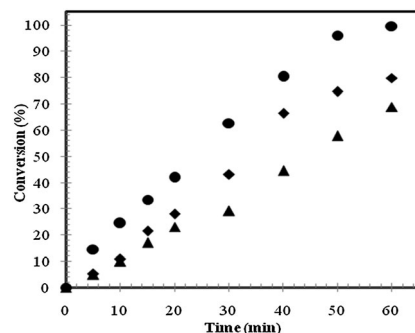


Fig. 8 Effect of mole ratio (3-(*O*-methylphenoxy)-1,2-propanediol: dimethyl carbonate). ▲ 1:6; ◆ 1:10; ● 1:15; reaction temperature: 140 °C; speed: 1000 rpm, catalyst loading: 0.03 g cm^{-3} .

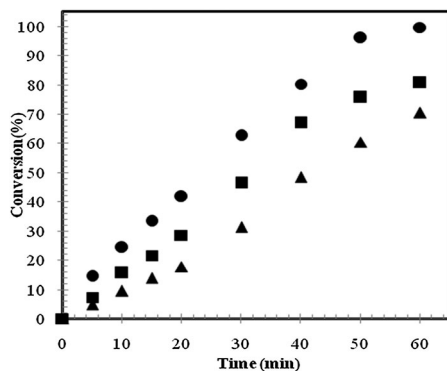
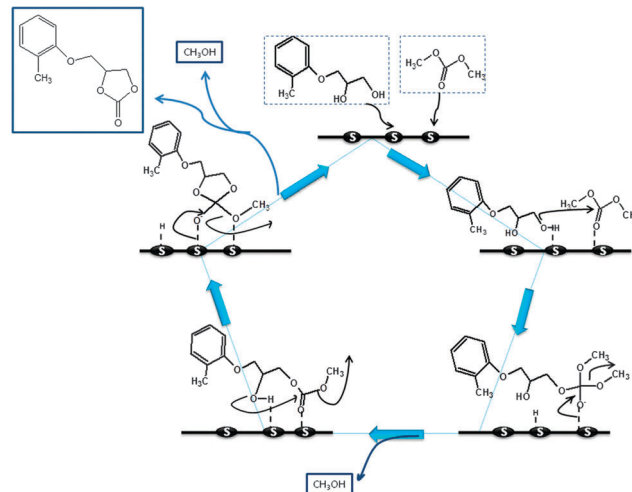


Fig. 9 Effect of temperature. ▲ 120 °C; ■ 130 °C; ● 140 °C, 3-(*O*-methylphenoxy)-1,2-propanediol, 3.6 g (0.02 mol); dimethyl carbonate: 27.04 g (0.3 mol), reaction temperature: 140 °C; catalyst loading: 0.03 g cm^{-3} .



Scheme 2 Proposed reaction mechanism.

reaction could be controlled by one of the following steps, namely: (a) adsorption, (b) surface reaction or (c) desorption. Therefore, the actual reaction mechanism was studied for the further development of the model.³⁸

The initial rate data can be analysed on the basis of the Langmuir–Hinshelwood–Hougen–Watson (LHHW) or the Eley–Rideal mechanism. From the initial rate, the following analysis was found to be the most appropriate. Scheme 2 was used to arrive at the LHHW type of mechanism with bifunctional sites

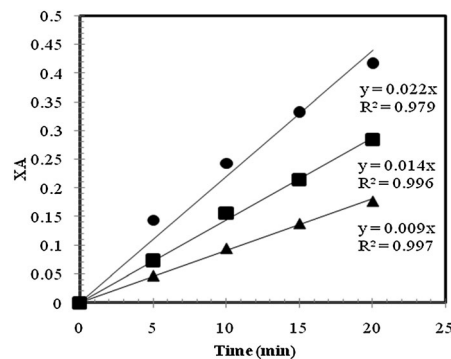


Fig. 10 Plots of X_A vs. time. ▲ 120 °C; ■ 130 °C; ● 140 °C.

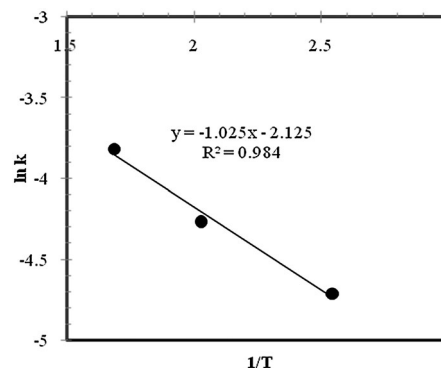


Fig. 11 Arrhenius plot.

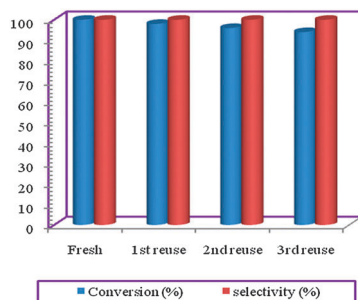


Fig. 12 Reusability study.

S_1 and S_2 . The preliminary analysis suggested that the reaction followed zero order kinetics.

The detailed reaction kinetics are elaborated in the ESI.† From the final equation the plots of X_A versus time were made

for a fixed value of w and C_{A0} to show a linear relation, where X_A is the fractional conversion of 3-aryl/alkyl-oxy-1,2-propanediol. The plots were constructed for different temperatures (Fig. 10). The slopes of these lines are equal to k_1 from which Arrhenius plots were constructed to determine the apparent energy of activation (Fig. 11). It was found to be $20.36 \text{ kcal mol}^{-1}$, which indicates that the reaction rate is intrinsically kinetically controlled.

Catalyst reusability

After the completion of the reaction, the catalyst was filtered and washed with dry methanol (50 cm^3) in order to remove adsorbed material from the catalyst surface and pores. It was then dried at $120 \text{ }^\circ\text{C}$ and calcined at $500 \text{ }^\circ\text{C}$ for 4 h in a nitrogen atmosphere. The catalyst lost during filtration was made up with fresh catalyst and activated and the activity was tested. The same conversion and selectivity was observed with the reused catalyst.

Table 4 Substrate study

Entry	Substrate (R)	Reaction time (h)	Solvent	Product	Conversion (%)	Selectivity (%)
1	2-Methylphenyl	1	— ^a		100	100
2	3-Methylphenyl	1	— ^a		100	100
3	4-Methylphenyl	1	— ^a		100	100
4	4-Methoxyphenyl	1	— ^a		100	100
5	Allyl	1.5	— ^a		100	100
6	2,5-Dichlorophenyl	3	MeOH		99	100
7	2,6-Dichlorophenyl	3	MeOH		98	100

^a Methanol was added to solubilise reactant in reaction mixture. Reaction conditions: 3-(O-methylphenoxy)-1,2-propanediol: 3.6 g (0.02 mol); dimethyl carbonate: 27.04 g (0.3 mol); reaction temperature: $140 \text{ }^\circ\text{C}$; catalyst loading: 0.03 g cm^{-3} , speed: 1000 rpm.

This demonstrated that the catalyst was stable and retained its catalytic activity. The same procedure was followed thrice. The catalyst was found to be stable and reusable three times without any loss in activity (Fig. 12). There was no change in selectivity. Leaching of basic sites, if any, in the liquid phase was tested by stopping the reaction after 30 min and immediately quenching the reaction mixture, which was followed by centrifuging it. The separated clear supernatant reaction mixture was then charged in to the reactor and reaction was continued under the same conditions. There was practically no conversion during the next two hours which suggests that the catalyst was stable and there was no leaching of alkali metal into the reaction mass. Green chemistry aspects of the process are described briefly in the ESI.†

Substrate study

To explore the generality and scope of the catalyst for 4-*O*-aryl/alkyl-oxy-1,3-dioxolan-2-one synthesis, the reaction was examined with structurally diverse 3-aryl/alkyl-oxy-1,2-propanediols (Table 4). In all cases, the reaction proceeded cleanly and the desired 4-*O*-aryl/alkyl-oxy-1,3-dioxolan-2-one was obtained with high selectivity. In the case of some substrates, solvent was required so as to dissolve the reactants.

Conclusion

A green process for the synthesis of 4-*O*-aryl/alkyl-oxy-1,3-dioxolan-2-one was developed using a highly active alkali promoted alkaline earth metal oxide catalyst which was prepared by a combustion synthesis method. The effect of different promoters on the conversion of aryl/alkyl-oxy-1,2-propanediol to its carbonate derivative was studied and lithium was found to be the best among other alkali metal promoters. It was found that as Li⁺ loading increased, the crystalline size increased and the surface area decreased. The maximum surface area obtained was 145 m² g⁻¹ for 0.1 wt% CS-Li/MgO. The catalytic activity was found to be the maximum with 0.1 wt% of Li⁺ metal loading. The catalyst is nanocrystalline with a crystalline size of 9 nm. The catalyst as prepared was reusable several times. The green aspects of this process appeared to offer a more promising green alternative over the conventional processes. A variety of substrates were also studied.

Acknowledgements

GDY acknowledges support as J. C. Bose National Fellow from DST-GOI and from R. T. Mody distinguished Professor Endowment. PSS gratefully acknowledges the support provided by UGC-SAP (Green technology), India.

References

- 1 S. Jegham, A. Nedelec, Ph. Burnier, Y. Guminski, F. Puech, J. J. Koenig and P. George, *Tetrahedron Lett.*, 1998, **39**, 4453–4454.
- 2 C. Chen, Y. E. Hyung, D. R. Vissers and K. I. Amine, *US Pat.*, 7,026,074, 2006.
- 3 F. T. Cook, M. O. Nutt and H. H. Hsieh, *US Pat.*, 4,500,717, 1985.
- 4 S. Jegham, F. Puech, P. Burnier, D. Berthon and O. Leclerc, *US Pat.*, 5,696,146, 1997.
- 5 S. Jegham, F. Puech, P. Burnier, D. Berthon and O. Leclerc, *US Pat.*, 6,143,772, 2000.
- 6 K. Yaegashi, Y. Furukawa and H. Yoshimoto, *US Pat.*, 6,271,388 B1, 2001.
- 7 F. Lee, T. Huang and C. Chung, *European Pat.*, EP1391458 A3, 2003.
- 8 B. J. Ludwing and E. C. Piech, *J. Am. Chem. Soc.*, 1951, **73**(12), 5894–5894.
- 9 S. Masumi and S. Takeshi, *Bull. Chem. Soc. Jpn.*, 2004, **77**(6), 1217–1228.
- 10 G. Zappia, E. Gacs-Baitz, G. D. Monache, D. Misiti, L. Nevola and B. Botta, *Curr. Org. Synth.*, 2007, **4**, 81–135.
- 11 M. Kazutsugu, F. Seiji, S. Megumi and K. Hidehiko, *Bull. Chem. Soc. Jpn.*, 1996, **69**(10), 2977–2988.
- 12 M. M. Baizer, J. R. Clark and J. Swidinsky, *J. Org. Chem.*, 1957, **22**, 1595–1598.
- 13 Y. M. Beasley, V. Petrow, O. Steephenson and A. J. Thomas, *J. Pharm. Pharmacol.*, 1957, **9**, 10–19.
- 14 W. B. McDowell, *US Pat.*, US2813104, 1957.
- 15 O. Mitsuru and Y. Shuichi, *European Pat.*, 943612 A1, 1999.
- 16 L. Ming-Shiu, M. Chen-Chi, L. Miaw-Ling and C. Feng-Chih, *J. Polym. Sci., Part A: Polym. Chem.*, 1996, **34**(16), 3303–3312.
- 17 H. Mineko, O. Eiji, T. Masayuki, S. Kaoru and Y. Nobuyuki, *Japanese Pat.*, JP2001129397, 2001.
- 18 A. Takagaki, K. Iwatani, S. Nishimura and K. Ebitani, *Green Chem.*, 2010, **12**, 578–581.
- 19 J. R. Ochoa-Gómez, O. Gómez-Jiménez-Aberasturi, B. Maestro-Madurga, A. Pesquera-Rodríguez, C. Ramírez-López, L. Lorenzo-Ibarreta, J. Torrecilla-Soria and M. C. Villarán-Velasco, *Appl. Catal., A*, 2009, **366**, 315–324.
- 20 M. Malyaadri, K. Jagadeeswaraiyah, P. S. Sai Prasad and N. Lingaiah, *Appl. Catal., A*, 2011, **401**, 153–157.
- 21 K. C. Patil, *Chemistry of Nanocrystalline Oxide Materials*, World Scientific Publishing Co. Pvt. Ltd, 2008.
- 22 A. Civera and M. Pavese, *Catal. Today*, 2003, **83**, 199–211.
- 23 Q. G. Wang, R. R. Peng, C. R. Xia, W. Zhu and H. T. Wang, *Ceram. Int.*, 2008, **34**, 1773–1778.
- 24 G. D. Yadav, N. P. Ajgaonkar and A. Varma, *J. Catal.*, 2012, **292**, 99–110.
- 25 G. D. Yadav and B. A. Gawade, *Catal. Today*, 2013, **207**, 145–152.
- 26 G. D. Yadav and G. P. Fernandes, *Catal. Today*, 2013, **207**, 162–169.
- 27 J. I. Di Cosimo, V. K. Díez and C. R. Apesteguía, *Appl. Catal., A*, 1996, **137**, 149–166.
- 28 A. Jose, F. Patcas and M. D. Amiridis, *Appl. Catal., A*, 2010, **386**, 1–8.
- 29 L. Leveles, K. Seshan, J. A. Lercher and L. Lefferts, *J. Catal.*, 2003, **218**, 296–306.
- 30 A. Trionfetti, S. Crapanzano, I. V. Babich, K. Seshan and L. Lefferts, *Catal. Today*, 2009, **145**, 19–26.
- 31 J. I. Di Cosimo, V. K. Díez and C. R. Apesteguía, *Appl. Catal., A*, 1996, **137**, 149–166.

- 32 V. K. Díez, C. R. Apesteguía and J. I. Di Cosimo, *J. Catal.*, 2006, **240**, 235–244.
- 33 M. Vijayaraj and C. S. Gopinath, *J. Catal.*, 2006, **243**, 376–388.
- 34 C. Nagappa and G. T. Chandrappa, *Microporous Mesoporous Mater.*, 2007, **106**, 212–218.
- 35 B. M. Reddy, S. Ashoka, G. T. Chandrappa and M. A. Pasha, *Catal. Lett.*, 2010, **138**, 82–87.
- 36 S. M. Maliyekkal, Anshup, K. R. Antony and T. Pradeep, *Sci. Total Environ.*, 2010, **408**, 2273–2282.
- 37 G. Egri, A. Kolbert, J. Balint, E. Fogassy, L. Novak and L. Poppe, *Tetrahedron: Asymmetry*, 1998, **9**, 271–283.
- 38 P. S. Kumbhar and G. D. Yadav, *Chem. Eng. Sci.*, 1989, **44**, 2535–2544.
- 39 G. D. Yadav and A. D. Murkute, *Langmuir*, 2004, **20**, 11607–11619.
- 40 G. D. Yadav and S. Sengupta, *Org. Process Res. Dev.*, 2002, **6**, 256–262.
- 41 G. D. Yadav and M. S. Krishnan, *Ind. Eng. Chem. Res.*, 1998, **2**, 3358–3365.
- 42 G. D. Yadav and N. S. Doshi, *Catal. Today*, 2000, **60**, 363–373.
- 43 G. D. Yadav and N. S. Doshi, *Org. Process Res. Dev.*, 2002, **6**, 263–272.